Extended Scheme using Equivalent Dipoles for Characterizing Edge Currents Along a Finite Ground Plane

C. Obiekezie, D. W. Thomas, A. Nothofer, S. Greedy, L. R. Arnaut, and P. Sewell

Electrical Systems and Optics Research Division
University of Nottingham, Nottingham, UK
{eexcso, dave.thomas, angela.nothofer, steve.greedy, luk.arnaut, phil.sewell}@ nottingham.ac.uk
chijiokeobiekezie@gmail.com

Abstract ─ For the assessment of radiated fields, a simplified analytical solution that approximates the effects of the currents induced at the edges of a finite ground plane is presented. These edge currents are induced by the actual current sources on the plane. This method can be used in characterizing the electromagnetic (EM) emission from any practical PCB and avoids the need for using high-frequency techniques in evaluating effects due to diffraction.

Index Terms ─ Analytical solution, diffraction, edge currents, equivalent dipole model, and multipole expansion.

I. INTRODUCTION

The increasing complexities of electronic circuits and the need for a suitable way of characterizing their electromagnetic (EM) performance has become a major problem in electromagnetic compatibility (EMC). In this work, equivalent infinitesimal dipoles are used for characterizing the EM properties of a PCB. In [1-6] a similar principle was used to characterize emissions from radiating sources above an infinite ground plane. In [7-9], radiations from the edges of the PCB, which are due to the via transitions of high speed signals, have been identified as a significant contributor to the total emissions from the PCB at a given observation point. Also these edge radiations increases as the emission sources are located close to the edges of the PCB. This makes the techniques adopted in [1-6] insufficient in representing all the sources of emissions from a practical PCB of finite size and according to [10]

further deteriorates as the emission sources are located close to the edges. Therefore to develop a model that can fully represent a real life scenario, all the possible sources of the emissions in the PCB need to be taken into consideration. Often, this does not lead to a close form solution. In particular, this greatly increases the mathematical complexities in evaluating the contribution of diffraction to the total emission around a PCB finite ground plane. Though there are classical solutions that offer good approximation for diffraction problems [11, 12], however, they can be complicated analytically and often lead to a complex integral equations. In [13] a hybrid technique that is based on equivalent dipole model and numerical techniques was used to characterize emissions from an enclosure with an aperture.

The uniqueness of our approach is that it offers an analytical solution, based on the equivalent dipole model only, that can approximate the diffraction effects with sufficient degree of accuracy with less than -10dB error. In this approach, equivalent dipoles are aligned on and along the edges of the ground plane to emulate the radiation characteristics of the currents induced at these edges.

II. THEORY

A. Field equivalence principle

This approach is based on the field equivalence principle [14, 15] as introduced by Schelkunoff in 1936 [16] and is equivalent to Huygens' principle [17]. In this method, the actual sources are replaced by fictitious sources placed

on an arbitrary surface surrounding it, producing the same fields outside the bounding surface. The sources are equivalent *inside* a region insofar as they produce the same amount of fields inside that region.

The equivalent sources are now computed through Love's equivalent principle [18] and taking into consideration the boundary conditions for ideal conductor as,

$$\overrightarrow{J_{eq}} = \hat{n} \times H_1 \qquad (1)$$

$$\overrightarrow{M_{eq}} = \hat{n} \times E_1 \quad , \qquad (2)$$

where J_{eq} and M_{eq} are the equivalent electric and magnetic sources, respectively. From equations (1) and (2), only the tangential components of the electric, E_1 or the magnetic, H_1 fields are required in order to compute the equivalent sources (or fictitious currents). Furthermore, in our work, these sources are modeled as infinitesimal dipoles.

B. Multipole expansion of dipole

Through multipole expansion [19] a simple source, D can be approximately modeled by 3 orthogonal electric and (or) magnetic dipole,

$$D = \left(D_x, D_y, D_z \right) \qquad (3)$$

where D_x, D_y, and D_z are the 3 orthogonal dipoles along the x, y, and z coordinates. This has been applied in [20] and [21] and the agreement with measurements was good. The solution is further derived as follows:

The magnetic field H_e from an electric dipole is determined from equation (4),

$$H_e = \frac{1}{\mu} \nabla \times \vec{A} \qquad (4)$$

and for a magnetic dipole as

$$H_m = -j\omega F - \frac{j}{\omega\mu\varepsilon} \nabla \left(\nabla \cdot \vec{F} \right) , \qquad (5)$$

where $\vec{A}$ and $\vec{F}$ are the magnetic and electric vector potentials respectively and μ and ε the permeability and permittivity of the surrounding media, respectively. For an electric dipole at $\left(x_0, y_0, z_0\right)$ oriented along the z-axis, the magnetic $\left(x, y, z\right)$ field at a distance r is given by,

$$H_x = -p^z \frac{jke^{-jkr}}{4\pi r^2}\left[1 + \frac{1}{jkr}\right]\left(y - y_0\right) \qquad (6)$$

$$H_y = -p^z \frac{jke^{-jkr}}{4\pi r^2}\left[1 + \frac{1}{jkr}\right]\left(x - x_0\right) , \qquad (7)$$

$$H_z = 0. \qquad (8)$$

Whereas for a magnetic dipole at (x_0, y_0, z_0) oriented in the z-direction,

$$H_x = M^z \frac{jke^{-jkr}}{4\pi r^4}\left(x - x_0\right)\left(z - z_0\right) \\ \left(jkr + 3 + \frac{3}{jkr}\right) \qquad (9)$$

$$H_y = M^z \frac{jke^{-jkr}}{4\pi r^4}\left(y - y_0\right)\left(z - z_0\right) \\ \left(jkr + 3 + \frac{3}{jkr}\right) , \qquad (10)$$

$$H_z = M^z \frac{jk^2 e^{-jkr}}{4\pi r}\left[\frac{(z-z_0)^2}{r^2}\left(j + \frac{3}{kr} + \frac{3}{jk^2 r^2}\right) - \left(j + \frac{3}{kr} + \frac{3}{jk^2 r^2}\right) \right] \qquad (11)$$

where p^z and M^z are the radiated electric and magnetic dipole moments, respectively. By taking into account the contributions from other dipole coordinates (x and y), we can formulate the relationship between the magnetic field and the dipole moments as,

$$\begin{bmatrix} H_x \\ H_y \\ H_z \end{bmatrix} = \begin{bmatrix} G_x^x & G_y^x & G_z^x \\ G_y^x & G_y^y & G_z^y \\ G_x^z & G_y^z & G_z^z \end{bmatrix} \begin{bmatrix} D_x \\ D_y \\ D_z \end{bmatrix} \qquad (12)$$

or, compactly,

$$[H] = [G][D] . \qquad (13)$$

In this approach, the field H is extracted from complete circuit through simulation or measurement. Therefore once the matrix G, which is a form of the dyadic Green's function is computed, the moment vector for the dipoles represented by D can then be solved through the solution to the inverse problem. This dipole moment vector can be electric, magnetic, or a combination of both.

C. Solution to inverse problem

In principle, a sufficient number of sampling points are required to properly compute the moments of the dipoles i.e.,

$$N^s \geq N^m,$$

where N^s and N^m are the total number of sampling points and dipoles, respectively. For

$$N^s = N^m,$$

the inverse problem involves a square matrix and basic techniques like Gaussian elimination can be used. But this becomes unfeasible as the size of the problem increases, thereby increasing the computational cost of this solution. In practice,

$$N^s \gg N^m,$$

leading to an over determined solution. Furthermore, as the positions of the infinitesimal dipoles are quite close, their dyadic Greens function with respect to the observation points are highly correlated. This accounts for the increase in the condition number of the matrix i.e.,

$$cond(A) = \infty .$$

For this reason, a more robust technique is required in solving this ill-posed and near singular inverse problem. So for a linear least square problem [22],

$$\min_{x} \|Ax - b\|_2, A \in R^{m \times n}, m > n \qquad (14)$$

the singular value decomposition (SVD) technique have been demonstrated to offer a unique solution for the inverse problem. The SVD of A is given by,

$$SVD(A) = U \sum V \qquad (15)$$

in such a way that they also satisfy,

$$A = U \sum V^T \qquad (16)$$

where $U(U^T U = I)$ and $V(V^T = V^{-1})$ are matrices with orthonormal columns and $\sum$ is a non-singular diagonal matrix.

In the previous work [1-3] where an infinite ground plane was assumed, only the direct and reflected fields were needed in computing the G matrix. This method achieved a good accuracy in general. However, this accuracy reduces significantly when using the above method to model sources above a finite plane and worsens as the sources are located closer to the edges of the plane. This is due to the scattering at the edges leading to diffractions, whence the image theory (used in approximating the effect of the ground plane) is no longer adequate because of the additional currents induced at the edges. To simplify this approach, a number of equivalent passive dipoles are placed around the edges of the ground plane to emulate the current induced at these edges due to the active sources on the structure. Therefore, the total field, H_T at any observation point is assumed to be a result of the contributions from the passive, H_{edge} and active dipoles, H_{source}. The set of passive dipoles are combined with the active dipoles (i.e., representing the active sources) to generate the dipole vector required for the model. Their relationship with the total field, H_T is formulated as,

$$H_T = H_{source} + H_{edge} \qquad (17)$$

$$[H_T] = [G][D_{source}] + [G][D_{edge}], \qquad (18)$$

$$H_T = [G]([D_{source}] + [D_{edge}]) . \qquad (19)$$

The expression in equation (19) is comparable to equation (13) where D comprises the D_{source} and the D_{edge}. The model for the active dipoles comprises the direct wave and its image while the passive dipoles are modeled in free space. To show the viability of this approach, a simple PCB tract comprising, a simple copper strip (L shape transmission line) is simulated on a dielectric over a finite ground plane. This approach was used to reproduce the fields from the structure at the simulated planes and also predict fields at other planes.

III. SIMULATION PROCEDURE

A. Diffraction effects

In addition to the model used in [1, 2], the finiteness of a ground plane also results to scattering at its edges. These scattering are due to currents induced at the edges of the ground plane by the actual electromagnetic (EM) sources on the device under test (DUT). This is also known as diffraction. This diffraction effects if ignored as in [1-6], degrades the performance of the equivalent dipole modeling (EDM) especially when the EM sources are located closer to the edges. Furthermore, to evince this effect, a rectangular PCB, with a simple L trace of 30mm × 70mm, was simulated using an MoM-based numerical code [23]. Firstly, the simple L trace was positioned at the centre of a large perfect electric conducting (PEC) ground plane with dimension 100mm ×

160mm as shown in Fig. 1 (a). This is then repeated with the L trace positioned close to the bottom-right of the PEC as shown in Fig. 1 (b). A dielectric surface of the same dimension as the PEC ($\varepsilon = 4.6$) with a thickness of 1.5 mm was placed in between the trace and the PEC to represent the typical FR4 properties. Figure 1 shows the physical layout of the two cases being considered here.

For uniformity, the same discretisation as shown was used and the trace was excited with 8dBmW signal at the shorter leg while the longer leg was terminated with a 50 Ω load in both cases. The load termination ensured continuous wave propagation in one direction. The transverse magnetic field computation in the xy-plane was carried out over a range of frequencies. For consistency, the same sampling resolution and sampling height of 4 mm and 10 mm, respectively were maintained for both cases.
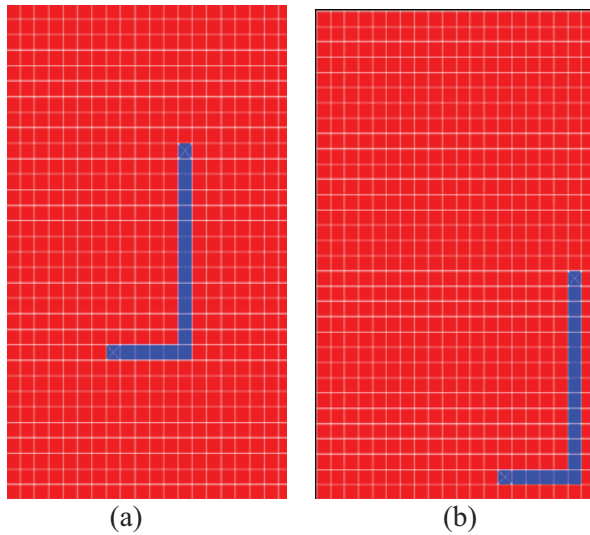

(a)   (b)

Fig. 1. Physical layout of a simple PCB with an L trace positioned at different locations above its dielectric layer.

This sampling resolution required was deduced from the expression [24],

$$\Delta s = \frac{\lambda}{2\sqrt{1+\left(\frac{\lambda}{d}\right)^2}} . \qquad (20)$$

This was also found to be sufficient for the frequency range considered in this experiment. The transverse fields were then imported into the dipole model and were used to determine the moment vector for the equivalent dipoles required to reproduce the same fields. Similar to the approach in [1, 2], the emission of the EM sources were characterized using a number of infinitesimal dipoles, with 10 mm uniform separation, whose images accounted for the reflection due to the PEC. For the two cases, the same number of dipoles and dipole resolution were used. This is to enable clear comparison as the error in equivalent dipole modeling tends to reduce with the increase in the number of dipoles.

Figure 2 compares the error in reproducing the transverse magnetic fields using EDM for the two cases shown in Fig. 1. The error significantly increases in case 2 (i.e., Fig. 1 (b)) and has been shown to be consistent for all the frequencies considered in this problem. The error was computed as the average of the r.m.s error, ζ in reproducing the two transverse fields as given in the expression,

$$\zeta = \sqrt{\frac{\sum_{i=1}^{N}\left(H_i^s - H_i^m\right)^2}{\sum_{i=1}^{N} H_i^{s^2}}} \qquad (21)$$

where H_i^s, H_i^m, and N are the magnetic fields from the numerical code, magnetic field reproduced using the EDM and the total number of sampling points, respectively. This increase in error, as the excited trace or the current sources are located close to the edge is often observed in complex PCBs due to diffraction. This error increases as the number of these sources increase in such a way that the image of the active sources are no longer sufficient to accurately characterize all the scattering effects due to the electric conducting ground plane. Edge dipoles are then introduced as passive sources to emulate the behaviors of the currents induced at the edges of the PEC ground plane by the actual sources. Again, to clearly distinguish the contributions of these passive dipoles from active dipoles used to characterize the active sources, another experiment was carried out.

B. Passive dipoles

To understand the influence of the passive dipoles, the same fields as in the two problems in section III were modeled using the EDM. However, unlike in the previous modeling, a number of infinitesimal dipoles were then introduced and positioned at the edges of the PEC

ground plane. Sufficient number is required so as to fully emulate the current excitation at the edges. Here infinitesimal dipoles of 10mm uniform separation was used. This is in addition to the number of infinitesimal dipoles of 10mm uniform separation, used previously to characterize the actual sources.
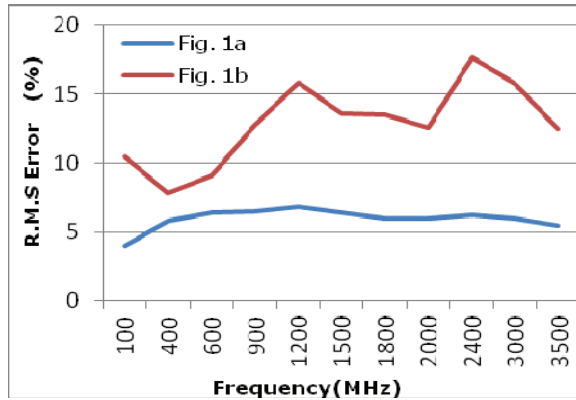

Fig. 2. R.M.S error for the different positions of the L trace.

It is necessary to distinguish the influence of the edge dipoles from just any additional dipole used for characterizing the active sources. It is expected that the increase in the number of dipoles reduces the error. However, it is important to show that the edge dipoles particularly represent the effects due to diffraction hence will only improve cases that are affected by diffraction.

The transverse magnetic fields were computed at the xy-plane for the two cases. These were then reproduced using the EDM with the additional active and passive dipoles. This implies that in addition to the number of active dipoles used in characterizing these problems previously, different dipoles (i.e., 52 passive dipoles, 31, 42, 64 active dipoles) were then added to highlight their contributions.

In case 1, the trace is located at the middle of the large ground plane with a good isolation from the edges. It is assumed that through this, there is minimal current induced at the edges of the ground plane due to the trace. Figure 3 shows the percentage improvement in the predicted transverse fields for 3 different numbers of active dipoles and also the case where passive dipoles are included. It is shown that addition of passive dipoles does not have much effect as compared

with the addition of active dipoles. This is because the greater proportion of the sources of the EM emissions are located on the surface of the PCB,

$$improvment = \frac{r.m.s_1 - r.m.s_2}{r.m.s_1} \times 100\%$$

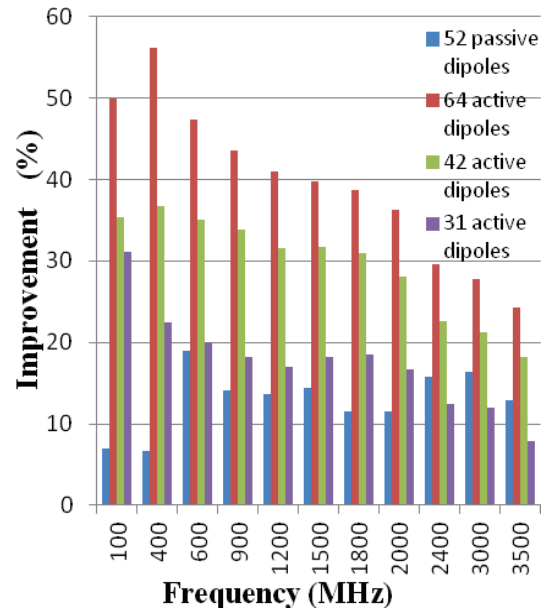where $r.m.s_1$ and $r.m.s_2$ are the error without and with additional dipoles, respectively.

Fig. 3. R.M.S improvement in reproducing case 1 by the addition of more dipoles (passive or active).

Conversely, Fig. 4 shows the results for case 2. A significant improvement is observed for the addition of passive dipoles. Unlike case 1, there is a significant amount of current induced at the edges of the ground plane. This was as a result of moving the L trace close to the right right-angular edge of the ground plane as shown in Fig. 1 (b). Hence, we can deduce from this that these edge dipoles can sufficiently emulate the induced currents at the edges. However, for case 2 additional active dipoles only had quite small an effect. This is because the active dipoles, which are positioned in such a way to characterize the actual sources of the emissions, cannot sufficiently emulate the behaviors of the additional currents induced at the edges of the ground plane. It has been shown that whilst the active dipoles can sufficiently characterize sources isolated from the edges of a ground plane, their performance declines as the sources are located closer to the

edge of the ground plane. The active sources with their images are used to characterize the direct radiation of EM sources including the scattering by PEC ground plane leading to reflection. This is sufficient for an infinite ground plane problem and can also give good results for problems with the EM sources well isolated from the edges of the ground plane. However, for a more realistic scenario in complex PCB designs, passive dipoles are introduced along the edges of the ground plane. This is to emulate the effects of edge currents leading to diffraction due to the finiteness of practical PCBs.
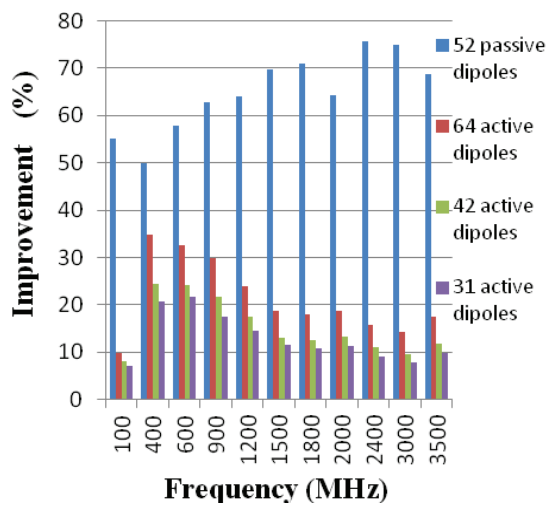

Fig. 4. R.M.S improvement in reproducing case 2 by the addition of more dipoles (passive or active).

C. Practical PCB

To further show the viability of this approach, a long metallic strip over a finite ground plane (160mm × 100mm) with similar EM performance as a practical PCB was simulated using MoM code [13]. Figure 5 (a) shows the physical design with 5mm mesh size and Fig. 1 (b) the current path along the L strip. The strip is excited with 8dBmW power at the tip of the shorter leg while the longer leg is terminated with a 50 Ω load. This simulation was carried out at 900 MHz and field results were extracted 10 mm above the planes. As given in equations (1) and (2), only the transverse fields are required in order to compute the equivalent currents. Unlike the problem treated earlier, the transverse fields on all the planes surrounding the PCB are required in the model. This is to provide sufficient information required to compute the

moments of the passive dipoles, which have been shown to contribute most to the diffracted fields. Samples taken from the xy-plane as used in sections III A) and III B) were sufficient because of the size of the trace and fewer edge current excitation is expected. However, for a larger trace located close to the edge, significantly more edge current excitation is expected and to properly characterize these edge currents, sufficient sampling around the PCB is required. The extracted complex-valued field are then imported into the equivalent dipole model of equation (13). The LHS of equation (13) comprises all the transverse fields extracted at each of the planes surrounding the structure. The first term on the RHS, which includes the direct, reflected, and diffracted field components, is then computed using equations (6) to (8) or equations (9) to (11) for electric or magnetic dipoles, respectively. The dipole moment vector is then calculated through the solution for the inverse problem.
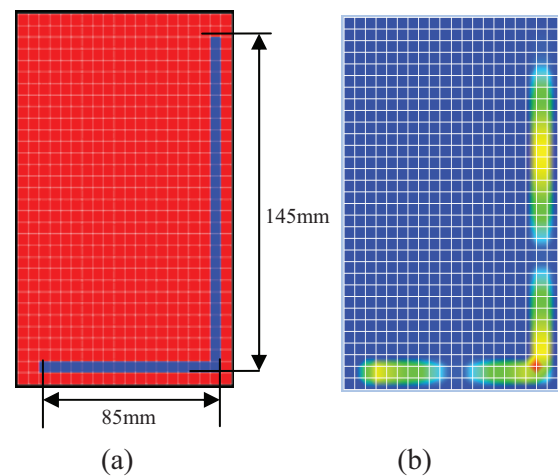

Fig. 5. (a) Physical design and (b) current path on the L-shape strip.

As described in section II C), the singular value decomposition technique was used. Following from the multipole expansion as also mentioned in section II B), 6 dipoles comprising 3 electric D_x^E, D_y^E, D_z^E and 3 magnetic D_x^M, D_y^M, D_z^M were first used to model each dipole point. This is computationally expensive and requires about 25 mins to run on an Intel core i7 3 GHz processor and 6 GB RAM PC. By trying different combination of dipoles and reducing the individual dipole moment redundancies, 3 orthogonal electric

dipoles were found to be sufficient in modeling the actual sources (active sources) while a combination of electric and magnetic dipoles were required for modeling the currents at the edges of the ground plane (passive sources). This is summarized as,

$$D_{active} = \begin{bmatrix} D_x^E \\ D_y^E \\ D_z^E \end{bmatrix} \qquad (22)$$

$$D_{passive} = \begin{bmatrix} D_x^E \\ D_y^E \\ D_z^M \end{bmatrix}. \qquad (23)$$

Though, any of the 3 orthogonal magnetic dipoles can equally be used in modeling the active sources with good accuracy, only the vertical magnetic dipoles can be used at the edges as the polarization of the horizontal magnetic dipole cannot generate currents in the direction of the actual currents induced at the edges. Initially, 468 dipoles were used, which takes approximately 5 minutes run time using the same PC. Figures 6 and 7 show the fields computed in the principal planes of the structure.
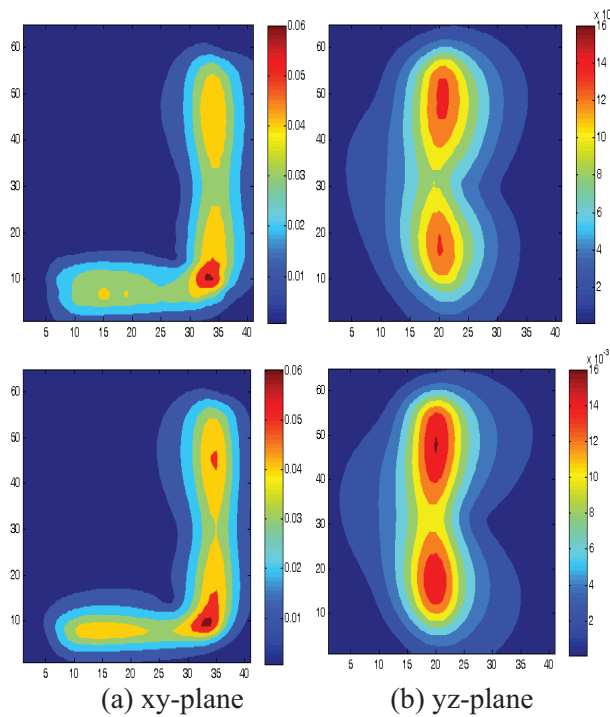

(a) xy-plane   (b) yz-plane

Fig. 6. Equivalent dipole model (1st row) and simulation (2nd row) of total magnetic field H_t, at 10 mm.

$H_T = \sqrt{H_x^2 + H_y^2 + H_z^2}$, also predictions were made at far-field distances from the structure using equivalent dipole model and results were compared with those from concept-II. These also show good agreement between the fields predicted with the equivalent dipole model and those computed using the MoM based concept-II software as shown in Fig. 8. Furthermore, by retaining only the dipole moments with significant contributions, $D_0 \left(i.e. \ D_0 \geq p \times D_{mMax} \right)$, to the total field observed at any given point, the total number of dipoles required for this model was reduced from 468 to 102, where D_{mMax} is the maximum dipole moment in the initial dipole moment vector and p is given proportion. Here we used a p value of 10 %. Figure 9 Shows the initial dipole and optimized final dipole positions on the surface of the structure. In Fig. 9 (b) the dipoles were found to be aligned along the current path as expected according to Fig. 5 (b). The moments of these optimized dipoles were then calculated according to equation (13) and used to predict these fields.
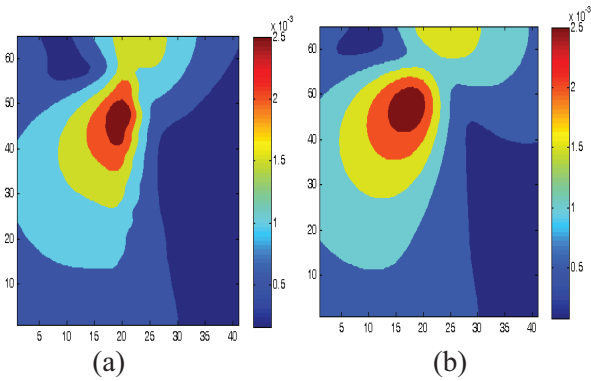

(a)   (b)

Fig. 7. (a) Equivalent dipole model and (b) simulation results of the total magnetic field H_T, at 10 mm for xz-plane.

The maximum difference between the two models is found for the top plane, because sufficient number of dipoles are required to accurately model the fields parallel to the surface of the large structure. Far-fields results for the different models were also computed. As shown in Fig. 8 (a) and (b), inclusion of the edge dipoles in the equivalent dipole model can closely predict radiations from finite structures in different EMC

environments. Dipole moments computed from the information obtained only from the top plane of the structure (i.e., xy-plane) results to higher error. This is represented by the magenta line. By including the field information from all planes surrounding the structure to compute the dipole moment, a more accurate prediction is observed as represented in green.
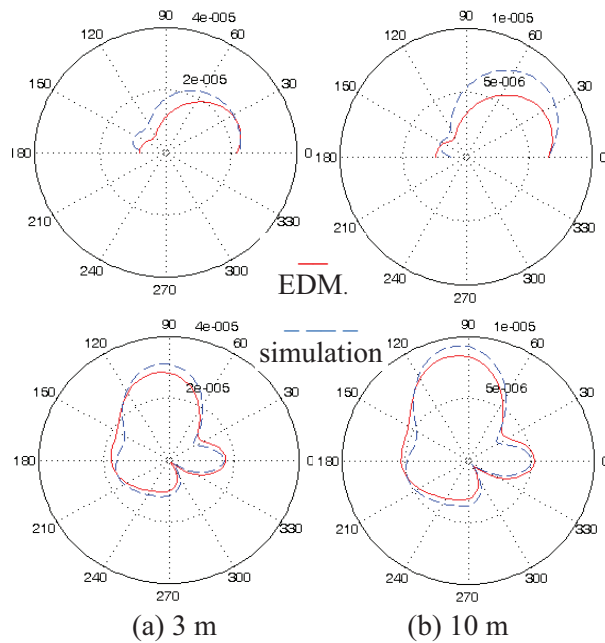

(a) 3 m   (b) 10 m

Fig. 8. H_θ (1st row) and H_ϕ (2nd row).
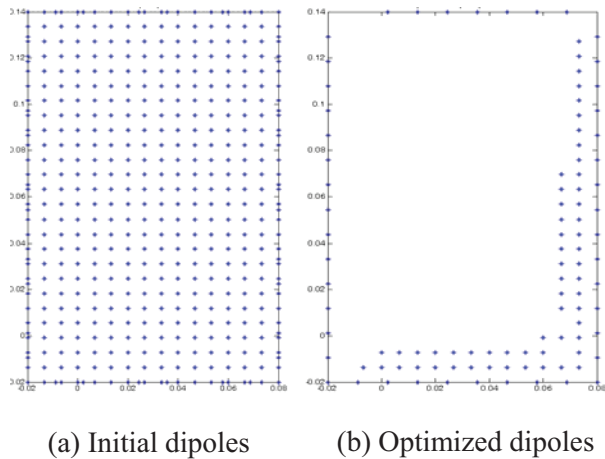

(a) Initial dipoles   (b) Optimized dipoles

Fig. 9. Dipoles positions on the plane.

This is quite similar to the results for 468 dipoles in Fig. 10, while the blue dash represents the simulated results in both cases. The maximum

fields at far-field regions 3 m and 10 m between 468 dipoles, 102 dipoles and numerical simulation also show a good agreement. Thus for this model, the specified degree of accuracy determines the number of dipoles to be used.
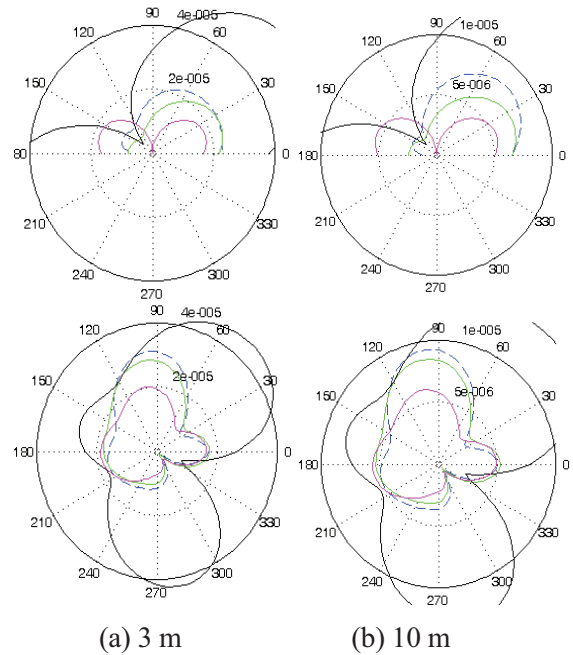

(a) 3 m   (b) 10 m

Fig. 10. H_θ (1st row) and H_ϕ (2nd row), { blue dash, green, magenta, and black}-{Simulation, 102 dipole model, dipole model with only top plane, dipole model without edge dipoles}.

IV. CONCLUSION

A scheme using equivalent dipoles to model radiated fields from complex radiators has been extended by including additional dipoles to represent diffraction effects. It is shown that a number of equivalent dipoles distributed along the edge of a finite ground can approximate the effects of the induced currents at its edges that leads to diffraction. The accuracy of this approach depends on the number of dipoles used. As this number increases, the time needed to evaluate the inverse problem increases correspondingly and can lead to ill-conditioning. However, techniques exist for solving ill-conditioned inverse problems. This approach will be used in the future work for predicting the coupling between different EM sources and their environments.

ACKNOWLEDGMENT

REFERENCES

[1] C. Obiekezie, D. Thomas, A. Nothofer, S. Greedy, and P. Sewell, "Electromagnetic characterization of 3D radiators," *EuroEM Conf.*, Toulouse, France, July 2012.

[2] X. Tong, D. Thomas, A. Nothofer, P. Sewell, and C. Christopoulos, "Modelling electromagnetic emissions from printed circuit boards in closed environments using equivalent dipoles," *IEEE Trans. Electromagn. Compat.*, vol. 52, no. 2, pp. 462-470, 2010.

[3] Y. Vives-Gilabert, C. Arcambal, A. Louis, F. de Daran, P. Eudeline, and B. Mazari, "Modeling magnetic radiations of electronic circuits using near-field scanning method," *IEEE Trans. Electromagn. Compat.*, vol. 49, no. 2, pp. 391-400, May 2007.

[4] L. Beghou, B. Liu, L. Pichon, and F. Costa, "Synthesis of equivalent 3-D models from near field measurements - Application to the EMC of power printed circuit boards," *IEEE Transactions on Magnetics*, vol. 45, no. 3, pp. 1650-1653, 2009.

[5] J.-R. Regué, M. Ribó, J.-M. Garrell, and A. Martín, "A genetic algorithm based method for source identification and far-field radiated emissions prediction from near-field measurements for PCB characterization," *IEEE Trans. Electromagn. Compat.*, vol. 43, no. 4, pp. 520-530, Nov. 2001.

[6] X. Tong, D. Thomas, A. Nothofer, P. Sewell, and C. Christopolous, "A genetic algorithm based method for modeling equivalent emission sources of printed circuits from near-field measurements," *Asia-Pacific International Symposium on Electromagn. Compat.*, Beijing, China, April 2010.

[7] J. Pak, H. Kim, J. Lee, and J. Kim, "Modeling and measurement of radiated field emission from a power/ground plane cavity edge excited by a through-hole signal via based on a balanced TLM and via coupling model," *IEEE Trans. on A dv. Packag.*, vol. 30, pp. 73-85, Feb. 2007.

[8] W. Cui, X. Ye, B. Archambeault, D. White, M. Li, and J. Drewniak, "EMI resulting from signal via transitions through the DC power bus," *IEEE International Symposium on Electromagnetic Compatibility*, pp. 821-826, 2000.

[9] H. Park, H. Jang, and H. Park, "Simulation and design of a PCB-chassis system for reducing radiated emissions," *Applied Computational Electromagnetics Society (ACES) Journal*, vol. 26, no. 8, pp. 679-687, August 2011.

[10] C. Obiekezie, D. Thomas, A. Nothofer, S. Greedy, L. Arnaut, and P. Sewell, "Optimization of equivalent dipole model to include edge effect," *ICEAA Conf.*, Torino, Italy, Sep. 2013.

[11] J. Keller, "Geometrical theory of diffraction," *J. Opt. Soc. Amer.*, vol. 52, no. 2, pp. 116-130, Feb. 1962.

[12] P. Ufimtsev, "Approximate computation of the diffraction of plane electromagnetic waves at certain metal bodies, Part I: Diffraction patterns at a wedge and a ribbon," *Soviet Phys.-Technical Phys.*, vol. 2, no. 8, pp. 1708-1718, Aug. 1957.

[13] C. Obiekezie, D. Thomas, A. Nothofer, S. Greedy, P. Sewell, and C. Christopoulos, "Prediction of emission from a source placed inside a metallic enclosure over a finite ground plane," *EMC Europe Conf.*, Rome, Italy, Sept. 2012.

[14] C. Balanis, *Advanced Engineering Electromagnetic*, Wiley, New York, 1989.

[15] C. Balanis, *Antenna Theory, Analysis and Design*, 3rd ed., Wiley, New Jersey, 2005.

[16] S. Schelkunoff, "Some equivalence theorems of electromagnetics and their application to radiation problems," *Bell Syst. Tech. J.*, vol. 15, pp. 92-112, 1936.

[17] C. Huygens, *Traite de la Lumiere,* S. P. Thompson, London, 1912.

[18] A. Love, "The integration of the equation of propagation of electric waves," *Phil. Trans. Roy. Soc. London*, *Ser.* A, vol. 197, pp. 1-45, 1901.

[19] J. Wikswo and K. Swinney, "Scalar multipole expansions and their dipole equivalents," *J. Appl. Phys.*, vol. 57, pp. 4301, 1985.

[20] P. Wilson, "On correlating TEM cell and OATS emission measurements," *IEEE Trans. Electromagn. Compat.*, vol. 37, no. 1, pp. 1-16, Feb. 1995.

[21] D. Geselowitz, "Multipole representations for an equivalent cardiac generator," *Proc. IRE*, vol. 48, pp. 75-79, Jan. 1960.

[22] P. Hansen, "Regularization tools: A Matlab package for analysis and solution of discrete ill-posed problems," *Numer. Algo.*, vol. 46, pp. 189-194, March 2008.

[23] Concept - II homepage, http://www.tet.tu-harburg.de/concept/index.en.html, 2012.

[24] E. Joy and D. Paris, "Spatial sampling and filtering in near-field measurements," *IEEE Trans. Antennas Propagat.*, vol. 20, pp. 253-261, May 1972.

Chijioke S. Obiekezie received the B.Eng. and M.Sc. degrees in Electrical and Electronic Engineering from the Federal University of Technology Owerri, Nigeria and Queen Mary University of London, U.K., in 2006 and 2009, respectively. He is currently working towards a Ph.D. degree in electrical and electronic engineering from the University of Nottingham, U.K.

David W. P. Thomas received the B.Sc. degree in physics from Imperial College of Science and Technology, London, U.K., the M.Phil. degree in space physics from Sheffield University, Sheffield, U.K., and the Ph.D. degree in Electrical Engineering from Nottingham University, Nottingham, U.K., in 1981, 1987, and 1990, respectively.

In 1990, he joined the Department of Electrical and Electronic Engineering, University of Nottingham, Nottingham, as a Lecturer, where he is currently a Professor of electromagnetic applications. His research interests include power system transients, power system protection, electromagnetic compatibility, and electromagnetic simulation.

Prof. Thomas is a member of International Council on Large Electric Systems and a Convenor for JWG 4.207.

Angela Nothofer was born in Uelzen, Germany, in 1967. She received the Dipl.-Ing. degree in Electrical Engineering from the University of Hannover, Hannover, Germany, in 1995,and the D.Phil. degree in Electronics from the University of York, York, U.K., in 2001.

In 2000, she joined the National Physical Laboratory, London, U.K., as a Member of the RF and Microwave Team, where she was engaged in developing standards and methods for measuring electromagnetic field strength. In 2005, she joined the George Green Institute for Electromagnetics Research, University of Nottingham, Nottingham, U.K., as a Lecturer in electromagnetic applications. Her current research interests include electromagnetic compatibility, and RF and microwave measurements using TEM waveguides, fully anechoic rooms, and reverberation chambers.

Stephen Greedy was born in Cardiff, U.K in 1966. He received the M.Eng. and Ph.D. degrees in Electrical and Electronic Engineering from the University of Nottingham, UK, in 1998 and 2002, respectively. The subject of his Ph.D. dissertation was the development and application of tools for the design of photonic integrated circuits and was titled "Advances in the Spectral Index Method for Optoelectronic design.". He was sponsored by DERA for the duration of his PhD. Following his Ph.D. he spent two years working as a research fellow on projects supported by Qinetiq and the Mobile telecommunications and health Research Programme.

He is a lecturer in the Department of Electrical and Electronic Engineering, University of Nottingham, UK. Research interests are in the area of computational electromagnetics, specifically the implementation of numerical algorithms on a variety of computational platforms and the simulation of systems for electromagnetic compatibility and signal integrity studies.

Luk R. Arnaut received the B.Sc. and M.Sc. degrees in Electrical and Electronic Engineering from the University of Ghent, Ghent, Belgium, in 1989, and the M.Sc. and Ph.D. degrees in Communication Engineering and Digital Electronics from the University of Manchester Institute of Science and Technology (UMIST), Manchester, U.K., in 1991 and 1994, respectively. From 1993 to 1994, he was a Research Associate at UMIST. During 1994, he was a Postdoctoral Research Scientist at the Defence Research Agency (now QinetiQ plc), Farnborough, U.K., where he was engaged in modeling, fabrication, and measurement of synthetic chiral composites. During 1995, he was a Visiting Scientist at the Naval Research Laboratory, Washington, DC. During 1995–1996, he was a Consultant at the Operations Division, British Aerospace plc (now BAE Systems), Bristol, U.K. From 1996 to 2010, he was a Senior Research Scientist at the National Physical Laboratory, Teddington, U.K., where he was a Key Scientific Advisor on mathematical modeling and the Lead Scientist of the Wireless Communications Science and Technology Group, within the Time, Quantum and Electromagnetics Division. Since 2008, he has been a Visiting Professor at the Imperial College of Science, Technology and Medicine, London, U.K. Since 2012, he has been a Research Fellow at the George Green

Institute for Electromagnetics Research at the University of Nottingham, U.K., where he is working on stochastic methods for analysis of circuits and complex sources. He is author or coauthor of more than 100 refereed publications, and holds two patents. His current research interests include electromagnetic interaction effects, statistical electromagnetics, complex media for radio-frequency and photonic applications (plasmonics), and multiple-input–multiple-output (MIMO) wireless communication systems.

Dr. Arnaut is the Convenor of the Joint Task Force on Reverberation chambers (JWG REV) between SC77B and CISPR/A of the International Electrotechnical Commissions, Geneva, Switzerland. He is a member of various past and present national and international networks, institutions, and steering groups. He is a Fellow of the Institution of Engineering and Technology. He is listed in *Who's Who in Science and Engineering*, *Who's Who in t he World*, and *International Biographical Centre's Cambridge Blue Book*.

Phillip Sewell received the B.Sc. (Hons.) degree in Electrical and Electronic Engineering and the Ph.D. degree from the University of Bath, Bath, U.K., in 1988 and 1991, respectively. From 1991 to 1993, he was a Postdoctoral Fellow with the University of Ancona, Ancona, Italy. In 1993, he was a Lecturer in the School of Electrical and Electronic Engineering, University of Nottingham, Nottingham, U.K., where he became a Reader and a Professor of electromagnetic, in 2001 and 2005.